

## Forbidden Rotational and Rovibrational Transitions in $\text{H}_3^+$ : First Principles Calculations

STEVEN MILLER AND JONATHAN TENNYSON<sup>1</sup>

*Department of Physics and Astronomy, University College London, Gower St., London WC1E 6BT, U.K.*

AND

BRIAN T. SUTCLIFFE

*Department of Chemistry, University of York, York YO1 5DD, U.K.*

Calculations of the linestrengths and transition frequencies of the forbidden pure rotational spectrum of  $\text{H}_3^+$  in the vibrationally excited  $\nu_2$  state are presented. These transitions occur in the far-infrared region, and their observation may be complicated by  $\nu_1 - \nu_2$  difference transitions. Examples of these are also given. Forbidden rovibrational transition frequencies and linestrengths have also been calculated in the frequency range 2000–3000  $\text{cm}^{-1}$ . The bands  $(\nu_2 + \nu_1) - \nu_2$  and  $(2\nu_2 (l = 0) + \nu_1) - 2\nu_2 (l = 2)$  are found to be particularly strong. Possible phenomenological explanations for the observed line intensities are discussed. Two routes to obtaining the energy levels of the  $\nu_1$  manifold of  $\text{H}_3^+$  are suggested. © 1990 Academic Press, Inc.

### 1. INTRODUCTION

Over the past few years, first principles calculations of the rovibrational energy levels and wavefunctions of the simple molecular ion  $\text{H}_3^+$  have proved remarkably successful (1). Not only have existing infrared transitions in the  $\nu_2$  fundamental manifold been reproduced with great accuracy (2), but hot band (3) and overtone (4) frequencies have been predicted and matched with unassigned experimental data (4, 5). The latter have proved important in the first-ever detection of  $\text{H}_3^+$  outside of the laboratory, in the atmosphere of Jupiter (6).

Two factors have contributed to this success. First, we have been able to use an extremely accurate potential energy surface, due to Meyer *et al.* (MBB) (7). Second, the two-step variational technique developed by Tennyson and Sutcliffe (8) has proved very efficient and well adapted to take the maximum advantage of advances in supercomputer technology (9).

Recently a number of workers have developed programs for calculating linestrengths, as well as transition frequencies, using dipole surfaces obtained ab initio (10, 11). Our TRIATOM program suite (12) has also been extended to compute linestrengths and stick spectra (13). Our codes have been benchmarked with those of Carter *et al.* and the results from both program suites shown to be in perfect agreement (14).

<sup>1</sup> Electronic mail addresses: SM7 and JT at UK.AC.RL.IB.

For triatomic molecules it is therefore clear that energy levels, transition frequencies, and linestrength/intensity data computed from first principles techniques can be relied on to give accurate results—*within the limitations of the potential energy and dipole surfaces employed.*

The general advantage that all first principles techniques enjoy over phenomenological methods of computing rovibrational energy levels is that the kinetic energy operator in the Hamiltonian is exact. It does not rely on second-order perturbation treatments. In the particular approach developed by Sutcliffe and Tennyson (15), the co-ordinate system is completely generalized and is not restricted to “small” displacements from a notional equilibrium geometry.

These advantages make our technique very useful for calculations involving “floppy” molecules, such as  $\text{H}_3^+$ , for which large-amplitude motions are important. Under such circumstances existing phenomenological Hamiltonians (16) need constant refinement and extension (17, 18). Even so, they begin to fail for energy levels which involve higher angular momentum states or for which other vibrational states cause large perturbations.

Another advantage of the first principles approach is that one may compute dipole transition moments between wavefunctions without making any a priori assumptions about which transitions are allowed and which “forbidden.” In fact, the reverse procedure may be adopted.

In our approach (19), there is absolutely no vibrational preassignment—the rovibrational energy levels computed are fully coupled. Assignment of the energy levels can then be made after they are computed on the basis of symmetry, energy ordering, and linestrength criteria.

In other words, the program suite is given no information about vibrational selection rules. It is simply given the task of calculating the rovibrational wavefunctions and then computing transition frequencies and linestrengths from these eigenfunctions.

The test of the program is that expected selection rules, derived under the rigid-rotor/harmonic-oscillator approximation, are obeyed to the same extent that they are obeyed by the experimental data. To this extent our calculations have proved successful (2).

The challenge of the calculations is that new phenomena may be predicted, as yet experimentally undetected, or that explanations may be provided for existing experimental data which have hitherto remained intractable to current theory. It is this aspect of the computation of  $\text{H}_3^+$  rovibrational transitions which we report in this paper.

## 2. COMPUTATIONAL DETAILS

Details of the calculations of rovibrational energy levels and linestrengths using the TRIATOM program suite (13) have been given in Ref. (3) and are not reported here. Absolute intensities are given assuming a Boltzmann distribution of the rovibrational energy levels at 300 K; i.e., we have not tried to separate off the vibrational contribution to the energy before weighting. This means that all the absolute intensities are very small. In practice,  $\text{H}_3^+$  may be produced vibrationally hot, giving greater absolute intensities than our calculations suggest.

In addition, in order to calculate the partition function from our data we have first computed its value assuming the spin weightings of all levels to be the 4, and then multiplied this value by  $\frac{2}{3}$  to allow for the fact that while there are roughly twice as many  $E$  states as  $A_2$  states, their spin weighting is only 2 compared with  $A_2$  states which have  $g_{ns} = 4$ . In this way, we obtain a value for the partition function of  $H_3^+$  at 300 K of 37.7.

This means that while the relative strengths of the transitions we report are correct, the absolute values should be accurate to about 10%. At higher temperatures, however, our method should become considerably more accurate.

Some idea of the relative strengths of vibrational manifolds may be obtained by looking at the absolute transition moment,  $M_{if}$ , computed for the equivalent of the ( $J' = 1, K' = 1 - J'' = 0, K'' = 0$ ) transition, which gives  $\partial\mu/\partial q$ , the transition dipole moment, for the vibration concerned. (This transition may not always be experimentally observable due to nuclear spin statistics, but it is always calculable.) Values of  $M_{01}$  for a number of bands are given in Table I.

### 3. FAR-INFRARED TRANSITIONS

Although  $H_3^+$  does not have a permanent dipole moment, there are two mechanisms by which it might exhibit a pure rotational spectrum. The first, proposed by Watson in 1971 (20), involves the distortion of the molecule as a result of centrifugal forces. Linestrengths are given by

TABLE I  
Absolute Transition Moments,  $M_{01}$ , for  $H_3^+$

Vibrational band	$M_{01}$ Debye	$\omega_{if}$ ( $\text{cm}^{-1}$ )
$\nu_2$ rotational	$5.9 \times 10^{-3}$	26.758
$\nu_1 - \nu_2$	0.068	719.536
$\nu_2 - \nu_0$	0.226	2627.183
$2\nu_2(l=0) - \nu_2$	0.131	2319.953
$2\nu_2(l=2) - \nu_2$	0.234	2603.227
$\nu_2 + \nu_1 - \nu_1$	0.245	2475.436
$\nu_2 + \nu_1 - \nu_2$	0.053	3062.527
$2\nu_2(l=2) - \nu_0$	0.089	4998.416
$3\nu_2(l=1) - \nu_2$	0.072	4524.387
$3\nu_2(l=+3) - \nu_0$	0.088	4804.675
$3\nu_2(l=-3) - \nu_0$	0.061	5050.684
$2\nu_2(l=2) + \nu_1 - \nu_1$	0.089	4700.481

$$S(f-i) = \frac{1}{4}(\theta_x^{xx})^2 \times F(J'K'J''K''). \quad (1)$$

Pan and Oka (henceforth PO) have calculated a value of  $\theta_x^{xx} = 1.08 \times 10^{-3}$  Debye for H<sub>3</sub><sup>+</sup> in its vibrational ground state (21). They also give explicit expressions for the  $F(J'K'J''K'')$ , derived from Watson's original paper (20, 21). Subsequent first principles variational calculations by Jensen and Spirko (10) and Miller and Tennyson (2) gave results of similar magnitude, although generally somewhat smaller, for the resulting linestrengths for a number of transitions.

The Watson formulation allows only  $\Delta K = 3$  transitions, with transitions from  $K = 1$  to  $K = 2$  and *vice versa*, being considered as transitions from  $K = -1$  to  $K = +2$ , thus fulfilling the  $\Delta K = 3$  requirements. This restriction, however, accounts for the fact that  $M_{01}$  for the ground state pure rotations is not reported, since the lowest combination of  $J$  levels for which a  $\Delta K = 3$  transition can occur is from  $J = 1$  to 2.

The second, although earlier mechanism, proposed by Mills, Watson, and Smith in 1969 (22) (henceforth MWS), explains the possibility of rotational transitions in degenerate levels of symmetric molecules via a vibrationally induced dipole moment. PO have also evaluated this for the degenerate  $\nu_2$  mode of H<sub>3</sub><sup>+</sup> (21). In this paper we present our variationally calculated values of transition frequencies and linestrengths.

At first sight, it might seem best to focus attempts to measure the rotational spectrum of H<sub>3</sub><sup>+</sup> in the far-infrared region on the ground state rotational transitions induced by Watson's centrifugal distortion mechanism. Recent studies of the infrared spectrum, however, by Xu *et al.* (5) have reported a number of hot band transitions. It is clear that the normal discharge methods of producing H<sub>3</sub><sup>+</sup> result in a significant population of vibrationally excited levels.

PO reformulated the MWS expression for pure rotational linestrengths in the  $\nu_2$  manifold. They obtained

$$\mu_{22} = \frac{\partial^2 \mu}{\partial q_2^2} - \frac{\phi_{222}}{\nu_2} \frac{\partial \mu}{\partial q_2}, \quad (2)$$

where  $q_2$  is the dimensionless  $\nu_2$  normal coordinate and  $\phi_{222}$  is the cubic anharmonicity term obtained from

$$\phi_{222} = \frac{1}{2} \left( \frac{\nu_2}{B} \right)^{3/2} q, \quad (3)$$

with  $B$  the ground state rotational constant and  $q$  the  $l$ -doubling constant.

Empirical data (17) combined with the constants derived from the CP dipole surface (23) gave a value for  $\mu_{22}$  of  $-5.2 \times 10^{-3}$  Debye, in good agreement with the value obtained from the  $M_{01}$  absolute transition moment of  $5.9 \times 10^{-3}$  Debye computed in this work.

Labeling of rovibrational states in H<sub>3</sub><sup>+</sup> (1) involves defining  $G = K - l_2$ , where  $l_2$  is the vibrational angular momentum quantum number normally associated with the degenerate  $\nu_2$  mode, and can take a value of  $-v_2, -(v_2 - 2), \dots, (v_2 - 2), v_2$ , where  $v_2$  is the number of quanta of  $\nu_2$  in the manifold. A parameter is then defined as  $U = -l_2$ , such that  $G = K + U$ . It is clear that for the  $\nu_2$  manifold,  $K$  states give rise to  $G = K + 1$  and  $G = K - 1$  levels.

TABLE II  
 "Forbidden" Rotational Transitions in  $\nu_2$

$J', G'_{v'} - J'', G''_{v''}$	$E'$ ( $\text{cm}^{-1}$ )	$E''$ ( $\text{cm}^{-1}$ )	$\omega_{if}$ ( $\text{cm}^{-1}$ )	$S(f-i)^a$ ( $\text{D}^2$ )	$I_{Ab}(\omega)^b$ 300K
2, 1 <sub>-1</sub> - 3, 4+1	2755.291	2719.308	35.983	0.291(-03)	0.707(-28)
5, 5+1 - 4, 2-1	3299.725	3259.663	40.061	0.958(-03)	0.214(-28)
1, 1+1 - 1, 2+1	2609.377	2548.041	61.337	0.564(-04)	0.853(-27)
5, 1 <sub>-1</sub> - 5, 2-1	3721.811	3659.563	62.247	0.337(-02)	0.254(-28)
4, 1 <sub>-1</sub> - 4, 2-1	3325.518	3259.663	65.854	0.106(-02)	0.604(-28)
2, 1+1 - 2, 2+1	2790.127	2723.765	66.363	0.519(-04)	0.391(-28)
4, 4+1 - 3, 1-1	3069.003	3002.486	66.517	0.462(-03)	0.920(-28)
3, 2 <sub>-1</sub> - 4, 5+1	2930.998	2863.711	67.287	0.573(-03)	0.227(-27)
5, 4 <sub>-1</sub> - 4, 1-1	3395.911	3325.518	70.393	0.105(-02)	0.492(-28)
3, 1 <sub>-1</sub> - 3, 2-1	3002.486	2930.998	71.488	0.207(-03)	0.662(-28)
5, 4+1 - 4, 1+1	3509.703	3422.758	86.946	0.770(-03)	0.333(-28)
4, 3 <sub>-1</sub> - 5, 6+1	3144.790	3047.090	97.701	0.102(-02)	0.663(-27)
5, 3+1 - 6, 6+1	3673.497	3568.950	104.547	0.101(-02)	0.301(-28)
5, 3 <sub>-1</sub> - 4, 0-1	3552.620	3446.685	105.935	0.379(-03)	0.416(-28)
2, 2+1 - 1, 1+1	2723.765	2609.377	114.387	0.386(-04)	0.135(-27)
4, 3 <sub>-1</sub> - 3, 0-1	3144.790	3025.528	119.263	0.677(-03)	0.691(-27)
7, 5 <sub>-1</sub> - 6, 2-1	4248.891	4128.273	120.618	0.751(-02)	0.296(-28)
5, 4 <sub>-1</sub> - 6, 7+1	3395.911	3269.207	126.704	0.176(-02)	0.309(-27)
3, 2+1 - 4, 5+1	2992.161	2863.711	128.450	0.652(-04)	0.820(-28)
3, 1+1 - 3, 2-1	3063.193	2930.998	132.195	0.954(-04)	0.913(-28)
3, 2 <sub>-1</sub> - 2, 1+1	2930.998	2790.127	140.871	0.790(-04)	0.166(-27)
3, 0 <sub>-1</sub> - 3, 3+1	3025.528	2876.591	148.937	0.782(-03)	0.239(-26)
6, 5 <sub>-1</sub> - 7, 8+1	3684.325	3529.762	154.563	0.290(-02)	0.204(-27)
6, 4+1 - 7, 7+1	4035.215	3876.409	158.806	0.210(-02)	0.295(-28)
6, 4 <sub>-1</sub> - 5, 1-1	3883.248	3721.811	161.438	0.332(-02)	0.100(-27)
4, 1+1 - 4, 2-1	3422.758	3259.663	163.094	0.243(-03)	0.687(-28)
6, 5+1 - 5, 2-1	3824.873	3659.563	165.310	0.593(-03)	0.251(-28)
6, 4+1 - 5, 1+1	4035.215	3862.944	172.271	0.329(-02)	0.563(-28)
3, 2 <sub>-1</sub> - 2, 1-1	2930.998	2755.291	175.707	0.404(-04)	0.145(-27)
7, 6 <sub>-1</sub> - 8, 9+1	4009.303	3828.412	180.891	0.465(-02)	0.204(-27)
5, 4+1 - 4, 1-1	3509.703	3325.518	184.185	0.332(-03)	0.833(-28)
4, 3+1 - 5, 6+1	3233.027	3047.090	185.937	0.228(-03)	0.444(-27)
5, 0 <sub>-1</sub> - 5, 3-1	3742.346	3552.620	189.726	0.505(-02)	0.896(-27)
4, 2 <sub>-1</sub> - 3, 1+1	3259.663	3063.193	196.471	0.156(-03)	0.153(-27)
2, 0 <sub>-1</sub> - 2, 3+1	2812.642	2614.135	198.508	0.250(-05)	0.429(-28)
6, 0 <sub>-1</sub> - 6, 3+1	4400.486	4201.773	198.712	0.705(-02)	0.599(-28)
5, 1+1 - 5, 2-1	3862.944	3659.563	203.381	0.336(-03)	0.200(-28)
8, 7 <sub>-1</sub> - 9, 10+1	4370.203	4164.763	205.440	0.729(-02)	0.390(-28)
2, 1 <sub>-1</sub> - 1, 2+1	2755.291	2548.041	207.250	0.249(-04)	0.315(-27)
4, 3+1 - 3, 0-1	3233.027	3025.528	207.499	0.297(-03)	0.761(-27)

<sup>a</sup> Powers of ten in brackets.

<sup>b</sup> Units  $\text{cm}^3/\text{molecule}$ .

TABLE II—Continued

$J', G'_{v_2} - J'', G''_{v_2}$	$E'$ ( $\text{cm}^{-1}$ )	$E''$ ( $\text{cm}^{-1}$ )	$\omega_{if}$ ( $\text{cm}^{-1}$ )	$S(f-i)^a$ ( $D^2$ )	$I_{\text{obs}}(\omega)^b$ 300K
5, 1 <sub>-1</sub> - 5, 4+1	3721.811	3509.703	212.108	0.130(-02)	0.169(-27)
4, 0 <sub>-1</sub> - 4, 3+1	3446.685	3233.027	213.658	0.472(-03)	0.469(-27)
5, 3 <sub>+1</sub> - 4, 0-1	3673.497	3446.685	226.813	0.213(-02)	0.836(-27)
7, 4 <sub>-1</sub> - 6, 1-1	4419.204	4187.703	231.500	0.477(-02)	0.275(-28)
5, 2 <sub>-1</sub> - 4, 1+1	3659.563	3422.758	236.806	0.181(-03)	0.424(-28)
3, 2 <sub>+1</sub> - 2, 1-1	2992.161	2755.291	236.870	0.325(-04)	0.187(-27)
5, 4 <sub>+1</sub> - 6, 7+1	3509.703	3269.207	240.496	0.519(-03)	0.261(-27)
4, 1 <sub>-1</sub> - 4, 4+1	3325.518	3069.003	256.514	0.709(-03)	0.103(-26)
4, 2 <sub>-1</sub> - 3, 1-1	3259.663	3002.486	257.177	0.276(-03)	0.551(-27)
7, 4 <sub>+1</sub> - 6, 1+1	4635.325	4377.784	257.541	0.880(-02)	0.241(-28)
3, 1 <sub>-1</sub> - 2, 2+1	3002.486	2723.765	278.721	0.502(-04)	0.431(-27)
3, 1 <sub>-1</sub> - 3, 4+1	3002.486	2719.308	283.178	0.169(-03)	0.151(-26)
6, 3 <sub>-1</sub> - 5, 0-1	4029.071	3742.346	286.725	0.590(-02)	0.797(-27)
4, 2 <sub>+1</sub> - 3, 1+1	3351.023	3063.193	287.831	0.211(-03)	0.373(-27)
6, 5 <sub>+1</sub> - 7, 8+1	3824.873	3529.762	295.111	0.995(-03)	0.195(-27)
7, 1 <sub>-1</sub> - 7, 4-1	4719.008	4419.204	299.804	0.765(-02)	0.215(-28)
4, 0 <sub>-1</sub> - 4, 3-1	3446.685	3144.790	301.894	0.166(-03)	0.425(-27)
6, 2 <sub>-1</sub> - 6, 5+1	4128.273	3824.873	303.400	0.205(-02)	0.101(-27)
6, 1 <sub>-1</sub> - 6, 4-1	4187.703	3883.248	304.455	0.463(-02)	0.173(-27)
3, 2 <sub>-1</sub> - 2, 3+1	2930.998	2614.135	316.863	0.290(-05)	0.507(-28)
5, 1 <sub>-1</sub> - 5, 4-1	3721.811	3395.911	325.899	0.111(-02)	0.477(-27)
4, 1 <sub>-1</sub> - 3, 2+1	3325.518	2992.161	333.357	0.154(-03)	0.473(-27)
5, 2 <sub>-1</sub> - 4, 1-1	3659.563	3325.518	334.045	0.947(-03)	0.588(-27)
3, 1 <sub>+1</sub> - 2, 2+1	3063.193	2723.765	339.428	0.115(-04)	0.131(-27)
6, 1 <sub>+1</sub> - 6, 4+1	4377.784	4035.215	342.569	0.247(-02)	0.528(-28)
3, 1 <sub>+1</sub> - 3, 4+1	3063.193	2719.308	343.884	0.267(-04)	0.317(-27)
4, 2 <sub>+1</sub> - 3, 1-1	3351.023	3002.486	348.537	0.147(-04)	0.457(-28)
7, 6 <sub>+1</sub> - 8, 9+1	4177.240	3828.412	348.829	0.171(-02)	0.203(-27)
5, 1 <sub>+1</sub> - 5, 4+1	3862.944	3509.703	353.241	0.717(-03)	0.199(-27)
4, 1 <sub>+1</sub> - 4, 4+1	3422.758	3069.003	353.754	0.147(-03)	0.339(-27)
5, 2 <sub>-1</sub> - 5, 5+1	3659.563	3299.725	359.839	0.115(-02)	0.893(-27)
5, 2 <sub>+1</sub> - 4, 1+1	3792.568	3422.758	369.811	0.113(-02)	0.508(-27)
5, 1 <sub>-1</sub> - 4, 2+1	3721.811	3351.023	370.788	0.120(-03)	0.760(-27)
6, 0 <sub>-1</sub> - 6, 3-1	4400.486	4029.071	371.415	0.986(-03)	0.485(-28)
7, 3 <sub>-1</sub> - 7, 6+1	4561.507	4177.240	384.267	0.351(-02)	0.889(-28)
7, 3 <sub>+1</sub> - 6, 0-1	4793.041	4400.486	392.556	0.159(-01)	0.141(-27)
4, 1 <sub>-1</sub> - 3, 2-1	3325.518	2930.998	394.520	0.990(-04)	0.512(-27)
4, 2 <sub>-1</sub> - 4, 5+1	3259.663	2863.711	395.952	0.228(-03)	0.164(-26)
8, 7 <sub>+1</sub> - 9, 10+1	4566.471	4164.763	401.708	0.277(-02)	0.395(-28)
6, 2 <sub>-1</sub> - 5, 1-1	4128.273	3721.811	406.462	0.215(-02)	0.261(-27)

Transition frequencies and linestrengths for the  $\nu_2$  pure rotational manifold between 0 and  $500 \text{ cm}^{-1}$  are given in Table II. The MWS theory predicts that  $\Delta G = 3$  transitions only ought to be allowed and this is borne out by our calculations. The other prediction

TABLE II—Continued

$J', G'_{U'} - J'', G''_{U''}$	$E'$ ( $\text{cm}^{-1}$ )	$E''$ ( $\text{cm}^{-1}$ )	$\omega_{if}$ ( $\text{cm}^{-1}$ )	$S(f-i)^a$ ( $D^2$ )	$I_{Abs}(\omega)^b$ 300K
3, 0 <sub>-1</sub> - 2, 3+1	3025.528	2614.135	411.393	0.212(-04)	0.106(-26)
7, 2 <sub>-1</sub> - 7, 5-1	4662.536	4248.891	413.645	0.764(-02)	0.760(-28)
4, 1 <sub>+1</sub> - 3, 2+1	3422.758	2992.161	430.597	0.265(-03)	0.115(-26)
6, 2 <sub>-1</sub> - 6, 5-1	4128.273	3684.325	443.948	0.201(-02)	0.327(-27)
6, 2 <sub>+1</sub> - 5, 1+1	4308.765	3862.944	445.821	0.306(-02)	0.212(-27)
6, 3 <sub>-1</sub> - 6, 6+1	4029.071	3568.950	460.121	0.200(-02)	0.119(-26)
5, 1 <sub>-1</sub> - 4, 2-1	3721.811	3259.663	462.147	0.413(-03)	0.543(-27)
5, 1 <sub>+1</sub> - 5, 4-1	3862.944	3395.911	467.033	0.120(-03)	0.813(-28)
7, 2 <sub>-1</sub> - 6, 1-1	4662.536	4187.703	474.832	0.448(-02)	0.720(-28)
6, 2 <sub>+1</sub> - 6, 5+1	4308.765	3824.873	483.892	0.778(-03)	0.720(-28)
4, 2 <sub>+1</sub> - 4, 5+1	3351.023	2863.711	487.312	0.113(-03)	0.106(-26)
5, 2 <sub>+1</sub> - 5, 5+1	3792.568	3299.725	492.844	0.271(-03)	0.319(-27)
6, 1 <sub>+1</sub> - 6, 4-1	4377.784	3883.248	494.536	0.438(-03)	0.315(-28)

of the theory, however, that transitions from  $U$  to  $-U$  ought to be favored, does not seem to be so rigorously adhered to. This is probably a result of the coupling between  $J, G_{+U}$  and  $J, G_{-U}$  states.

The dipole moment  $M_{01}$  for the transition from  $\nu_2$  to  $\nu_1$  is more than an order of magnitude greater than that for the  $\nu_2$  pure rotational transition (Table I). Linestrengths and intensities for the difference band, given in Table III, indicate that from around  $200 \text{ cm}^{-1}$  onward these lines are likely to dominate the far-infrared spectrum of vibrationally hot transitions. This effect can be seen clearly in Fig. 1, where we have simulated a stick spectrum of the hot transitions in the region from 0 to  $300 \text{ cm}^{-1}$  at a temperature of 300 K.

(The difference band linestrengths are not, however, sufficient for them to be observed under conditions of a spectrum derived from a complete Boltzmann distribution of rovibrational levels: in that case only the pure rotational spectrum of ground state  $\text{H}_3^+$  is likely to be measured.)

#### 4. FORBIDDEN ROVIBRATIONAL TRANSITIONS

Rovibrational eigenfunctions, frequencies, and linestrengths for  $\text{H}_3^+$ , computed in the  $2000\text{--}3000 \text{ cm}^{-1}$  region, include several transitions which involve a change of 1 in the  $\nu_1$  quantum number. On the basis of rigid-rotor/harmonic-oscillator selection rules such transitions should be forbidden, since  $\partial\mu/\partial q_1$  is zero. Nonetheless, these transitions have significant linestrengths and are therefore considered to be possible candidates for observation.

The extent to which these transitions may be important can be gauged from Table I, showing the transition moments. For the  $\nu_2$  fundamental,  $M_{01}$  is 0.226 Debye. By comparison, we compute a mere  $3.4 \times 10^{-6}$  Debye for the highly forbidden  $\nu_1$  tran-

TABLE III  
Difference Band Transitions from  $\nu_2$  to  $\nu_1$

$J', K' - J'', G''_{v''}$	$E'$ ( $\text{cm}^{-1}$ )	$E''$ ( $\text{cm}^{-1}$ )	$\omega_{if}$ ( $\text{cm}^{-1}$ )	$S(f - i)^a$ ( $D^2$ )	$I_{Ab,}(\omega)^b$ 300K
5, 4 - 6, 4 <sub>+1</sub>	4084.430	4035.215	49.215	0.249(-01)	0.200(-28)
5, 5 - 6, 5 <sub>+1</sub>	3888.463	3824.873	63.590	0.123(-01)	0.437(-28)
4, 1 - 5, 1 <sub>+1</sub>	3991.586	3862.944	128.641	0.328(-01)	0.344(-27)
4, 2 - 5, 2 <sub>+1</sub>	3927.953	3792.568	135.384	0.294(-01)	0.470(-27)
6, 6 - 7, 6 <sub>-1</sub>	4146.689	4009.303	137.386	0.511(-01)	0.595(-27)
6, 5 - 7, 5 <sub>-1</sub>	4388.877	4248.891	139.986	0.300(-01)	0.571(-28)
4, 3 - 5, 3 <sub>+1</sub>	3820.625	3673.497	147.128	0.226(-01)	0.148(-26)
6, 4 - 7, 4 <sub>-1</sub>	4575.494	4419.204	156.290	0.195(-01)	0.198(-28)
4, 4 - 5, 4 <sub>+1</sub>	3667.003	3509.703	157.300	0.113(-01)	0.907(-26)
5, 4 - 6, 4 <sub>-1</sub>	4084.430	3883.248	201.181	0.255(-01)	0.509(-27)
5, 3 - 6, 3 <sub>-1</sub>	4232.349	4029.071	203.279	0.142(-01)	0.287(-27)
5, 5 - 6, 5 <sub>+1</sub>	3888.463	3684.325	204.138	0.447(-01)	0.237(-26)
5, 2 - 6, 2 <sub>-1</sub>	4336.643	4128.273	208.370	0.583(-02)	0.380(-28)
3, 0 - 4, 0 <sub>-1</sub>	3682.614	3446.685	235.929	0.269(-01)	0.112(-25)
3, 1 - 4, 1 <sub>+1</sub>	3660.983	3422.758	238.226	0.253(-01)	0.600(-26)
3, 2 - 4, 2 <sub>+1</sub>	3595.663	3351.023	244.640	0.200(-01)	0.693(-26)
3, 3 - 4, 3 <sub>+1</sub>	3485.273	3233.027	252.246	0.100(-01)	0.129(-25)
4, 3 - 5, 3 <sub>-1</sub>	3820.625	3552.620	268.005	0.182(-01)	0.552(-26)
4, 2 - 5, 2 <sub>-1</sub>	3927.953	3659.563	268.389	0.772(-02)	0.707(-27)
4, 1 - 5, 1 <sub>-1</sub>	3991.586	3721.811	269.775	0.185(-02)	0.126(-27)
4, 4 - 5, 4 <sub>-1</sub>	3667.003	3395.911	271.092	0.362(-01)	0.119(-25)
3, 1 - 4, 1 <sub>-1</sub>	3660.983	3325.518	335.465	0.267(-02)	0.167(-26)
3, 2 - 4, 2 <sub>-1</sub>	3595.663	3259.663	336.000	0.112(-01)	0.960(-26)
3, 3 - 4, 3 <sub>-1</sub>	3485.273	3144.790	340.482	0.270(-01)	0.819(-25)
2, 1 - 3, 1 <sub>+1</sub>	3409.833	3063.193	346.640	0.179(-01)	0.412(-25)
2, 2 - 3, 2 <sub>+1</sub>	3343.175	2992.161	351.014	0.933(-02)	0.307(-25)
2, 1 - 3, 1 <sub>-1</sub>	3409.833	3002.486	407.347	0.434(-02)	0.167(-25)
2, 2 - 3, 2 <sub>-1</sub>	3343.175	2930.998	412.176	0.175(-01)	0.960(-25)
1, 0 - 2, 0 <sub>-1</sub>	3263.187	2812.642	450.544	0.150(-01)	0.327(-24)
1, 1 - 2, 1 <sub>+1</sub>	3240.819	2790.127	450.692	0.918(-02)	0.111(-24)
1, 1 - 2, 1 <sub>-1</sub>	3240.819	2755.291	485.528	0.817(-02)	0.129(-24)

<sup>a</sup> Powers of ten in brackets.

<sup>b</sup> Units  $\text{cm}/\text{molecule}$ .



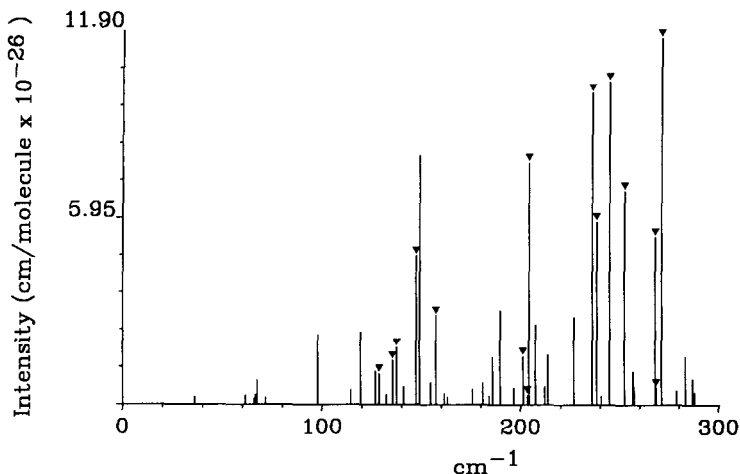


FIG. 1. Simulated far-infrared spectrum of  $\text{H}_3^+$  at 300 K, showing  $\nu_2$  rotational transitions and the  $\nu_1 - \nu_2$  difference band (labelled ▼). Intensities are computed assuming a Boltzmann distribution of the rovibrational energy levels (see text).

sition. But for  $(\nu_2 + \nu_1) - \nu_2$ —essentially a  $\nu_1$  hot transition— $M_{01}$  is  $5.3 \times 10^{-2}$  Debye, comparable to the  $2\nu_2$  overtone value of  $8.9 \times 10^{-2}$  Debye (Table I).

Results for the  $(\nu_2 + \nu_1) - \nu_2$  manifold are given in Table IV. The lines given in this table were chosen on the basis of having a Boltzmann weighted intensity of at least 1% of the strongest  $2\nu_2 - \nu_2$  hot band transition at 300 K. The transitions given in Tables V to IX were selected on the same basis with respect to the  $3\nu_2 - 2\nu_2$  manifold. This is in line with the selection procedure used in Ref. (3).

It is clear from Tables IV–IX that among the allowed hot band transitions a number of “forbidden” rovibrational lines may be found. We estimate that the calculated frequencies ought to be about  $0.6 \text{ cm}^{-1}$  too low for the  $(\nu_2 + \nu_1) - \nu_2$  manifold, and around  $1 \text{ cm}^{-1}$  too low for the other bands, in line with our previous calculations (3).

The transitions in Tables IV–IX all show the  $\Delta G$ ,  $G - K$ , or  $K - G = 3$  behavior that would be expected from the MWS mechanism rather than the strict  $\Delta K = 3$  behavior exhibited by the centrifugally induced dipole mechanism of Watson (20). An initial attempt to calculate the magnitude of this effect from

$$\mu_{221} = \frac{\partial \mu_{22}}{\partial q_1} q_1 \quad (4)$$

produced a result of just 0.013 Debye, only 25% of the computed value of  $M_{01}$  of 0.053 Debye for the  $(\nu_2 + \nu_1) - \nu_2$  manifold.

Thus it is clear that a more sophisticated approach to a phenomenological interpretation of these transitions is necessary, such as that outlined by Aliev and Watson

TABLE IV  
 "Forbidden" Transitions from  $\nu_2$  to  $\nu_2 + \nu_1$

$J', G'_{U'} - J'', G''_{U''}$	$E'$ ( $\text{cm}^{-1}$ )	$E''$ ( $\text{cm}^{-1}$ )	$\omega_{if}$ ( $\text{cm}^{-1}$ )	$S(f-i)^a$ ( $D^2$ )	$I_{Ab}(\omega)^b$ 300K
2, 3 <sub>+1</sub> - 3, 0 <sub>-1</sub>	5653.682	3025.528	2628.154	0.205(-2)	0.106(-24)
4, 5 <sub>+1</sub> - 4, 2 <sub>-1</sub>	5920.834	3259.663	2661.171	0.169(-1)	0.143(-24)
5, 5 <sub>+1</sub> - 5, 2 <sub>-2</sub>	6346.032	3659.563	2686.469	0.320(-1)	0.404(-24)
2, 2 <sub>+1</sub> - 3, 1 <sub>+1</sub>	5755.490	3063.193	2692.298	0.241(-2)	0.531(-25)
3, 4 <sub>+1</sub> - 3, 1 <sub>+1</sub>	5764.679	3063.193	2701.487	0.394(-2)	0.873(-25)
3, 4 <sub>+1</sub> - 3, 1 <sub>-1</sub>	5764.679	3002.486	2762.193	0.810(-2)	0.246(-24)
4, 4 <sub>+1</sub> - 4, 1 <sub>-1</sub>	6105.255	3325.518	2779.737	0.111(-1)	0.720(-25)
1, 2 <sub>+1</sub> - 2, 1 <sub>+1</sub>	5583.811	2790.127	2793.684	0.141(-2)	0.119(-24)
4, 3 <sub>+1</sub> - 4, 0 <sub>-1</sub>	6254.046	3446.685	2807.361	0.113(-1)	0.823(-25)
3, 0 <sub>-1</sub> - 4, 3 <sub>+1</sub>	6046.732	3233.027	2813.705	0.697(-2)	0.143(-24)
2, 1 <sub>+1</sub> - 3, 2 <sub>+1</sub>	5815.188	2992.161	2823.027	0.350(-2)	0.114(-24)
2, 3 <sub>+1</sub> - 2, 0 <sub>-1</sub>	5653.682	2812.642	2841.039	0.710(-2)	0.549(-24)
3, 3 <sub>+1</sub> - 3, 0 <sub>-1</sub>	5909.649	3025.528	2884.122	0.112(-1)	0.635(-24)
5, 6 <sub>+1</sub> - 4, 3 <sub>+1</sub>	6129.580	3233.027	2896.554	0.227(-1)	0.474(-24)
1, 1 <sub>+1</sub> - 2, 2 <sub>+1</sub>	5639.999	2723.765	2916.234	0.333(-2)	0.405(-24)
4, 5 <sub>+1</sub> - 3, 2 <sub>+1</sub>	5920.834	2992.161	2928.673	0.173(-1)	0.583(-24)
3, 2 <sub>+1</sub> - 3, 1 <sub>+1</sub>	6015.313	3063.193	2952.120	0.499(-2)	0.121(-24)
3, 1 <sub>-1</sub> - 4, 4 <sub>+1</sub>	6022.981	3069.003	2953.977	0.553(-2)	0.130(-24)
2, 0 <sub>-1</sub> - 3, 3 <sub>+1</sub>	5834.642	2876.591	2958.051	0.509(-2)	0.603(-24)
2, 2 <sub>+1</sub> - 2, 1 <sub>+1</sub>	5755.490	2790.127	2965.363	0.552(-2)	0.497(-24)
1, 2 <sub>+1</sub> - 1, 1 <sub>+1</sub>	5583.811	2609.377	2974.434	0.427(-2)	0.920(-24)
3, 4 <sub>+1</sub> - 2, 1 <sub>+1</sub>	5764.679	2790.127	2974.552	0.593(-2)	0.535(-24)
4, 2 <sub>-1</sub> - 5, 5 <sub>+1</sub>	6275.437	3299.725	2975.713	0.660(-2)	0.517(-25)
5, 6 <sub>+1</sub> - 4, 3 <sub>-1</sub>	6129.580	3144.790	2984.790	0.199(+0)	0.657(-23)
4, 5 <sub>+1</sub> - 3, 2 <sub>-1</sub>	5920.834	2930.998	2989.836	0.750(-1)	0.346(-23)
5, 5 <sub>+1</sub> - 4, 2 <sub>+1</sub>	6346.032	3351.023	2995.009	0.751(-1)	0.463(-24)
2, 2 <sub>+1</sub> - 2, 1 <sub>-1</sub>	5755.490	2755.291	3000.199	0.116(-2)	0.130(-24)

<sup>a</sup> Powers of ten in brackets.

<sup>b</sup> Units cm/molecule.

(24). Comparison of the Hamiltonian used in their approach and that used in our first principles calculations is extremely complicated, however, and we have not attempted such an analysis here.

TABLE V  
 "Forbidden" Transitions from  $2\nu_2(0)$  to  $2\nu_2(0) + \nu_1$

$J', K' - J'', K''$	$E'$ ( $\text{cm}^{-1}$ )	$E''$ ( $\text{cm}^{-1}$ )	$\omega_{if}$ ( $\text{cm}^{-1}$ )	$S(f-i)^a$ ( $\text{D}^2$ )	$I_{Ab,}(\omega)^b$ 300K
2, 1 - 3, 2	8014.243	5209.308	2804.936	0.630(-3)	0.491(-30)

<sup>a</sup> Powers of ten in brackets.

<sup>b</sup> Units  $\text{cm}/\text{molecule}$ .

### 5. CONCLUSIONS

First principles calculations of spectroscopic data are important because they allow the prediction of phenomena for which there exists no adequate phenomenological theory. The results we have reported for forbidden rotational and rovibrational transitions in  $\text{H}_3^+$  indicate that several lines may be observable.

As well as their intrinsic interest in themselves, forbidden transitions are known to play an important role in astrophysical processes, such as the cooling of the interstellar medium. Any experimental data on these lines would therefore be extremely welcome.

TABLE VI  
 "Forbidden" Transitions from  $2\nu_2(2)$  to  $2\nu_2(0) + \nu_1$

$J', K' - J'', G'' \nu''$	$E'$ ( $\text{cm}^{-1}$ )	$E''$ ( $\text{cm}^{-1}$ )	$\omega_{if}$ ( $\text{cm}^{-1}$ )	$S(f-i)^a$ ( $\text{D}^2$ )	$I_{Ab,}(\omega)^b$ 300K
2, 1 - 3, 2 <sub>+2</sub>	8014.243	5532.956	2481.287	0.226(-1)	0.330(-29)
1, 1 - 2, 2 <sub>+2</sub>	7841.529	5265.703	2575.826	0.104(-1)	0.566(-29)
1, 0 - 2, 3 <sub>+2</sub>	7859.324	5180.662	2678.663	0.290(-1)	0.495(-28)
2, 1 - 3, 4 <sub>+2</sub>	8014.243	5298.686	2715.557	0.134(-1)	0.656(-29)
2, 1 - 2, 2 <sub>+2</sub>	8014.243	5265.703	2748.540	0.385(-1)	0.224(-28)
1, 1 - 1, 2 <sub>+2</sub>	7841.529	5087.004	2754.525	0.253(-1)	0.348(-28)
1, 1 - 2, 4 <sub>+2</sub>	7841.529	5031.976	2809.553	0.119(-1)	0.217(-28)
1, 1 - 0, 2 <sub>+2</sub>	7841.529	4997.423	2844.106	0.178(-1)	0.389(-28)
1, 0 - 1, 3 <sub>+2</sub>	7859.324	4994.314	2865.010	0.267(-1)	0.119(-27)
2, 1 - 1, 2 <sub>+2</sub>	8014.243	5087.004	2927.240	0.276(-1)	0.403(-28)
2, 1 - 2, 4 <sub>+2</sub>	8014.243	5031.976	2982.267	0.703(-2)	0.136(-28)

<sup>a</sup> Powers of ten in brackets.

<sup>b</sup> Units  $\text{cm}/\text{molecule}$ .

<sup>c</sup> Intensity "stealing" from close-lying levels.

TABLE VII

"Forbidden" Transitions from  $2\nu_2(0)$  to  $2\nu_2(2) + \nu_1$ 

$J', G'_{v'} - J'', G''_{v''}$	$E'$ ( $\text{cm}^{-1}$ )	$E''$ ( $\text{cm}^{-1}$ )	$\omega_{if}$ ( $\text{cm}^{-1}$ )	$S(f-i)^a$ ( $D^2$ )	$I_{Ab_2}(\omega)^b$ 300K
$2, 4_{+2} - 3, 1$	7916.363	5280.799	2635.564	0.232(-2)	0.121(-29)
$2, 3_{+2} - 3, 0$	8058.213	5304.036	2754.177	0.819(-2)	0.796(-29)
$2, 4_{+2} - 2, 1^c$	7916.363	5022.056	2894.307	0.528(-2)	0.104(-28)
$1, 2_{+2} - 2, 1$	7963.841	5022.056	2941.784	0.372(-2)	0.747(-29)
$2, 1_{-2} - 3, 2$	8170.369	5209.308	2961.061	0.694(-2)	0.571(-29)

<sup>a</sup> Powers of ten in brackets.<sup>b</sup> Units  $\text{cm}/\text{molecule}$ .<sup>c</sup> Intensity "stealing" from close-lying levels.

Our data also suggest that there may be two routes by which the energy levels of the  $\nu_1$  manifold may be determined. The first method is by the measurement of the  $\nu_2$  to  $\nu_1$  difference band in the far-infrared region.  $\nu_2$  levels are known to very high

TABLE VIII

"Forbidden" Transitions from  $2\nu_2(2)$  to  $2\nu_2(2) + \nu_1$ 

$J', G'_{v'} - J'', G''_{v''}$	$E'$ ( $\text{cm}^{-1}$ )	$E''$ ( $\text{cm}^{-1}$ )	$\omega_{if}$ ( $\text{cm}^{-1}$ )	$S(f-i)^a$ ( $D^2$ )	$I_{Ab_2}(\omega)^b$ 300K
$2, 4_{+2} - 3, 1_{-2}^c$	7916.363	5485.152	2431.212	0.168(-1)	0.302(-29)
$1, 3_{+2} - 2, 0_{-2}$	7874.402	5285.893	2588.509	0.495(-2)	0.493(-29)
$1, 2_{+2} - 2, 1_{-2}$	7963.841	5304.112	2659.728	0.912(-3)	0.427(-29)
$0, 2_{+2} - 1, 1_{-2}$	7868.771	5124.508	2744.263	0.719(-3)	0.820(-30)
$2, 3_{+2} - 2, 0_{-2}$	8058.213	5285.893	2772.320	0.300(-2)	0.320(-29)
$2, 4_{+2} - 1, 1_{-2}^c$	7916.363	5124.508	2791.856	0.486(-3)	0.565(-30)
$1, 2_{+2} - 1, 1_{-2}$	7963.841	5124.508	2839.333	0.146(-2)	0.173(-29)
$2, 1_{-2} - 2, 2_{+2}$	8170.369	5265.703	2904.666	0.324(-2)	0.199(-29)
$1, 1_{-2} - 1, 2_{+2}$	7991.681	5087.004	2904.678	0.100(-2)	0.145(-29)
$1, 1_{-2} - 0, 2_{+2}$	7991.681	4997.423	2994.259	0.266(-3)	0.610(-30)

<sup>a</sup> Powers of ten in brackets.<sup>b</sup> Units  $\text{cm}/\text{molecule}$ .<sup>c</sup> Intensity "stealing" from close-lying levels.

TABLE IX  
 "Forbidden" Transitions from  $\nu_2 + \nu_1$  to  $\nu_2 + 2\nu_1$

$J', G'_{v'} - J'', G''_{v''}$	$E'$ ( $\text{cm}^{-1}$ )	$E''$ ( $\text{cm}^{-1}$ )	$\omega_{if}$ ( $\text{cm}^{-1}$ )	$S(f-i)^a$ ( $\text{D}^2$ )	$I_{Ab_s}(\omega)^b$ 300K
1, 2 <sub>+1</sub> - 1, 1 <sub>+1</sub>	8521.562	5639.999	2881.563	0.647(-2)	0.656(-30)
0, 1 <sub>+1</sub> - 1, 2 <sub>+1</sub>	8487.095	5583.811	2903.284	0.368(-2)	0.492(-30)
1, 0 <sub>-1</sub> - 2, 3 <sub>+1</sub>	8576.978	5653.682	2923.296	0.833(-2)	0.160(-29)
1, 2 <sub>+1</sub> - 0, 1 <sub>+1</sub>	8521.562	5553.712	2967.849	0.429(-2)	0.680(-30)
1, 1 <sub>+1</sub> - 1, 2 <sub>+1</sub>	8577.799	5583.811	2993.988	0.442(-2)	0.610(-30)

<sup>a</sup> Powers of ten in brackets.

<sup>b</sup> Units  $\text{cm}/\text{molecule}$ .

accuracy, and far-IR spectroscopy is also very precise. The drawback is that the measurement of ion spectra in this region is still comparatively difficult.

The second route involves the measurement of two bands— $(\nu_2 + \nu_1) - \nu_1$ , which has already been measured by Xu *et al.* (5), and  $(\nu_2 + \nu_1) - \nu_2$ . The energies of the upper  $(\nu_2 + \nu_1)$  levels could then be determined from  $\nu_2$ , and the  $\nu_1$  levels by subtraction.

It would be interesting to compare such essentially direct infrared measurements of the  $\nu_1$  manifold not only with those calculated from first principles (1, 3), but with indirect measurements of this level by vibrational autoionization of  $\text{H}_3$  (25, 26). The more accurate of these measurements agreed with our calculated value for the band origin of  $\nu_1$  of  $3178.35 \text{ cm}^{-1}$  to within experimental accuracy (25).

The data contained in Tables II to XI are limited for reasons of space, having been chosen on intensity criteria which we consider to be useful to experimentalists. We have, however, computed far more data than are reported here and are more than willing to supply any other transitions which may be required.

#### ACKNOWLEDGMENTS

The authors thank Professors Ian Mills and Takeshi Oka and Drs. James Watson and K. Sarka for helpful discussions during the preparation of this paper. We acknowledge the Science and Engineering Research Council for funding under Grants GR/E/98348 and GR/F/14550. All the calculations presented in this paper were carried out using the Cray XMP-48 computer at the RAL Atlas Centre.

RECEIVED: November 13, 1989

#### REFERENCES

1. S. MILLER AND J. TENNYSON, *J. Mol. Spectrosc.* **126**, 183-192 (1987).
2. S. MILLER AND J. TENNYSON, *Astrophys. J.* **335**, 486-490 (1988).
3. S. MILLER AND J. TENNYSON, *J. Mol. Spectrosc.* **136**, 223-240 (1989).

4. W. A. MAJEWSKI, J. K. G. WATSON, P. A. FELDMAN, S. MILLER, AND J. TENNYSON, *Astrophys. J.* **347**, L51–L54 (1989).
5. L. W. XU, M. G. BAWENDI, B. D. REHFUSS, C. GABRYS, AND T. OKA, 43rd Symposium on Molecular Spectroscopy, Columbus, Ohio, 1989, Paper RA3.
6. P. DROSSART, J.-P. MAILLARD, J. CALDWELL, S. J. KIM, J. K. G. WATSON, W. A. MAJEWSKI, J. TENNYSON, S. MILLER, S. ATREYA, J. CLARKE, J. H. WAITE JR., AND R. WAGENER, *Nature (London)* **340**, 539–541 (1989).
7. W. MEYER, P. BOTSCHWINA, AND P. G. BURTON, *J. Chem. Phys.* **84**, 891–900 (1986).
8. J. TENNYSON AND B. T. SUTCLIFFE, *Mol. Phys.* **58**, 1067–1081 (1986).
9. B. T. SUTCLIFFE, S. MILLER, AND J. TENNYSON, *Comput. Phys. Commun.* **51**, 73–82 (1988).
10. P. JENSEN AND V. ŠPIRKO, *J. Mol. Spectrosc.* **118**, 208–231 (1986).
11. S. CARTER, J. SENEKOWITSCH, N. C. HANDY, AND P. ROSMUS, *Mol. Phys.* **65**, 143–160 (1988).
12. J. TENNYSON, *Comput. Phys. Commun.* **42**, 257–270 (1986).
13. J. TENNYSON AND S. MILLER, *Comput. Phys. Commun.* **55**, 149–175 (1989).
14. S. CARTER, P. ROSMUS, N. C. HANDY, S. MILLER, J. TENNYSON, AND B. T. SUTCLIFFE, *Comput. Phys. Commun.* **55**, 71–75 (1989).
15. B. T. SUTCLIFFE AND J. TENNYSON, *Mol. Phys.* **58**, 1053–1066 (1986); *Int. J. Quantum Chem.*, in press (1990).
16. J. K. G. WATSON, *Mol. Phys.* **103**, 350–363 (1984).
17. J. K. G. WATSON, S. C. FOSTER, A. R. W. MCKELLAR, P. BERNATH, T. AMANO, F. S. PAN, M. W. CROFTON, R. S. ALTMAN, AND T. OKA, *Canad. J. Phys.* **62**, 1875–1885 (1984).
18. W. A. MAJEWSKI, M. D. MARSHALL, A. R. W. MCKELLAR, J. W. C. JOHNS, AND J. K. G. WATSON, *J. Mol. Spectrosc.* **122**, 567–582 (1987).
19. S. MILLER, J. TENNYSON, AND B. T. SUTCLIFFE, *Mol. Phys.* **66**, 429–456 (1986).
20. J. K. G. WATSON, *J. Mol. Spectrosc.* **40**, 536–544 (1971).
21. F. S. PAN AND T. OKA, *Astrophys. J.* **305**, 518–525 (1986).
22. I. M. MILLS, J. K. G. WATSON, AND W. L. SMITH, *Mol. Phys.* **16**, 329–344 (1969).
23. G. D. CARNEY AND R. N. PORTER, *J. Chem. Phys.* **60**, 4251–4264 (1974).
24. M. R. ALIEV AND J. K. G. WATSON, in “Molecular Spectroscopy, Modern Research” (K. Narahari Rao, Ed.), Vol. 3, pp. 1–67, Academic Press, San Diego, 1985.
25. W. KETTERLE, H.-P. MESSMER, AND H. WALTHER, *Europhys. Lett.* **8**, 333–338 (1989).
26. L. J. LEMBO, A. PETIT, AND H. HELM, *Phys. Rev. A* **39**, 3721–3724 (1989).